

# Differentiating pathologic parathyroid glands from thyroid nodules on neck ultrasound: the PARATH-US cross-sectional study



Dolly Yazgi,<sup>a</sup> Carine Richa,<sup>a</sup> Sylvie Salenave,<sup>a</sup> Peter Kamenicky,<sup>a</sup> Amel Bourouina,<sup>a</sup> Lorraine Clavier,<sup>b</sup> Margot Dupeux,<sup>c</sup> Jean-François Papon,<sup>d</sup> Jacques Young,<sup>a</sup> Philippe Chanson,<sup>a</sup> and Luigi Maione<sup>a,\*</sup>



<sup>a</sup>Université Paris-Saclay, Inserm, Physiologie et Physiopathologie Endocrinienne, Assistance Publique-Hôpitaux de Paris, Hôpital Bicêtre, Service d'Endocrinologie et des Maladies de la Reproduction, Le Kremlin-Bicêtre, France

<sup>b</sup>Department of Endocrinology, Melun Hospital, 77000, France

<sup>c</sup>Université Paris-Saclay, Assistance Publique-Hôpitaux de Paris, Hôpital Bicêtre Service d'Anatomie et Cytologie Pathologiques, Le Kremlin-Bicêtre, France

<sup>d</sup>Université Paris-Saclay, Assistance Publique-Hôpitaux de Paris, Hôpital Bicêtre, Service d'Oto-Rhino-Laryngologie et Chirurgie Cervico-Maxillo Faciale, Le Kremlin-Bicêtre, France

## Summary

**Background** Neck ultrasound (US) is a widely used and accessible operator-dependent technique that helps characterize thyroid nodules and pathologic parathyroid glands (PPGs). However, thyroid nodules may sometimes be confused with PPGs. PARATH-US study aims at identifying US characteristics to differentiate PPGs from thyroid nodules, as there is no study, at present, which directly compares the US features of these two common neoplasms.

**Methods** PARATH-US is a single-center study that was conducted at a tertiary referral center, including consecutive lesions from patients undergoing neck US examination from 2016 to 2022.

**Findings** 176 PPGs (158 patients: serum calcium levels 2.91 [IQR 2.74–3.05] mmol/L, PTH levels 173 [112–296] ng/L) were compared to 232 size- and volume-matched thyroid nodules (204 age- and sex-matched patients). The morphologic patterns, echoic content and vascular status were all different between PPGs and thyroid neoplasms ( $p < 0.01$  for all comparisons). The combined parameters maximally discriminated PPGs from thyroid nodules (OR, 7.6; 95% CI: 3.4, 17.1,  $p < 0.0001$ ). When applying risk stratification systems developed for thyroid malignancies, 58–63% of PPGs were classified as high-risk lesions. Parathyroid adenomas had larger sizes and volumes than hyperplasias ( $p = 0.013$  and  $p = 0.029$ ). Serum calcium and PTH levels were significantly correlated with PPG size and volume ( $p < 0.0001$  for all comparisons).

**Interpretation** We demonstrate the presence of distinct US characteristics in PPGs, which help differentiate them from thyroid nodules. When mistaken for thyroid nodules, PPGs bear high-risk US features. When dealing with high-risk cervical lesions detected on US, a PPG should be suspected, and an assessment of calcium levels recommended to avoid unnecessary invasive procedures.

**Funding** CYTO-TRAIN, C2022DOSRH053, funded by the French Regional Health Agency.

**Copyright** © 2023 The Author(s). Published by Elsevier Ltd. This is an open access article under the CC BY-NC-ND license (<http://creativecommons.org/licenses/by-nc-nd/4.0/>).

**Keywords:** Thyroid cancer; Hyperparathyroidism; Fine-needle aspiration; MEN1; Parathyroid hormone

## Introduction

Parathyroid and thyroid neoplasms are highly prevalent in the general population. Primary hyperparathyroidism is the most frequent cause of chronic calcium excess, and is related to the autonomous secretion of

parathyroid hormone (PTH) by one or multiple pathologic glands. If untreated, this disease may lead to nephrolithiasis and bone demineralization.<sup>1</sup> Parathyroid imaging is often demanded before surgery. Among available imaging techniques, almost every patient with

\*Corresponding author.

E-mail address: [luigi.maione@aphp.fr](mailto:luigi.maione@aphp.fr) (L. Maione).

### Research in context

#### Evidence before this study

Prior to the start of the PARATH-US, we performed an extensive literature review on observational studies, reviews and meta-analyses using PubMed, Embase, the Cochrane library database on studies published before December 2021 and searching for terms including “thyroid nodules”, and “hyperparathyroidism”, “parathyroid nodules”, “parathyroid gland ultrasonography” and “parathyroid adenoma”. We found a large number of studies focusing on US description, management, risk assessment and guidelines about thyroid nodules (n = 1224); conversely, only a few studies dealt with US or contrast-enhanced US description of PPGs (n = 39). However, a direct comparison of thyroid neoplasms and PPGs on US has never been conducted to date, despite the wide diffusion of US workstations.

#### Added value of this study

PARATH-US study directly compares PPGs and thyroid nodules. We demonstrate the presence of distinct US characteristics in PPGs, which help clinicians and US point-of-care practitioners to differentiate them from thyroid nodules. We provide novel information in subgroup of patients with different forms of hyperparathyroidism.

#### Implications of all the available evidence

Based on the results of the PARATH-US study, we expect that PPGs might be taken into account by US operators. As PPGs bear high-risk US features when confused with thyroid nodules, the assessment of phosphocalcic homeostasis should be recommended to avoid unnecessary invasive procedures.

hyperparathyroidism undergoes a first-line neck ultrasound (US) to concomitantly evaluate the thyroid status.<sup>2,3</sup> Parathyroid nodules on US are mainly reported as oblong and hypoechoic structures, generally located between the thyroid apex and the exterior branch of the superior laryngeal nerve (superior parathyroid glands) and close to the inferior thyroidal arteries (inferior parathyroid glands).<sup>4</sup> In several instances, however, pathologic parathyroid glands (PPGs) may be confused with thyroid nodules, demanding unnecessary cytology or even surgery.<sup>5</sup> On the other hand, thyroid nodules are highly prevalent in the general population and are thus frequently described during routine neck US exploration.<sup>6</sup> In this setting, US devices have been used to develop risk stratification systems (RSSs) to predict cancer risk and to establish the requirement to perform cytopathological analyses.<sup>7,8</sup> Being an inexpensive, noninvasive and nonirradiating imaging technique, neck US is widely used in various medical settings, including radiology, endocrinology, head and neck surgery, general and internal medicine.<sup>9,10</sup> When dealing with cervical lesion, discriminating thyroid from parathyroid lesions may thus be a challenging task for clinicians performing neck US. The aim of the present work was to compare the US characteristics of PPG to those of size-matched thyroid nodules. In addition, we provide descriptive analyses and bioradiological correlations in different subgroups of patients with PPGs.

## Methods

### Patients

PARATH-US is a single-center observational study that was conducted at a tertiary referral center (Department of Endocrinology and Reproductive Diseases, Bicetre University Hospital, France). This study involved consecutive neck US examinations in

patients with hyperparathyroidism (primary, secondary or tertiary) and in those with thyroid nodules performed from 2016 to 2022. The evidence of parathyroid origin came from histopathologic examinations and/or from a positive intranodular parathyroid hormone (PTH) measurement.<sup>11</sup>

We excluded patients with intellectual disabilities, those not understanding the protocol and those with no proof of parathyroid origin.

US characteristics of PPGs were compared to consecutive size- and volume-matched thyroid nodules analyzed in the same center over the same period.

The PARATH-US study was conducted in accordance with the Declaration of Helsinki. All patients were informed by a notice explaining the type of the study, its scopes and aims, the handling of sensitive confidential data with information about the right of opposition (according to the French Regulations on data protection, from the Commission Nationale de l'informatique et des libertés (CNIL), see also <https://www.cnil.fr/fr/les-bases-legales/consentement>). The PARATH-US study protocol has been scrutinized and approved by the local Ethics committee (Comité d'Evaluation Ethique de l'Institut National de la Santé et de la Recherche Médicale (INSERM) with the annotation CEEI no. 21–869 of 7 December 2021, Ref. CD/EB 21–159). In addition, information notices had been distributed and posted in public spaces of our department.

### Neck ultrasound examination

US examinations were conducted on Hitachi Aloka Arietta A70 (from 2016 to Apr. 2020) or Aloka Arietta A750 (from May 2020 onward) workstations (Hitachi Medical System SAS, Switzerland) by two experienced operators (CR and LM) by means of two electronic linear transducers (L64 transducer 38 mm, 5–18 MHz; and L55 transducer 50 mm, 5–15 MHz). Each patient was

examined in a supine position with neck hyperextension. US images were taken on the transverse and longitudinal sections. Vascular signals were analyzed by eFlow and DFI techniques.<sup>12</sup> Beyond the usual loges extending to the submental region downward until the brachiocephalic vessels, the examination was completed by a thorough exploration of the carotid spaces and lateral cervical regions.

The following parameters were collected and described: a) size (anteroposterior “x”, transverse “y”, and longitudinal “z”, in mm) and volume (using the formula  $[V = 4/3\pi * xyz/1000]$  (mm<sup>3</sup>), expressed in mL); b) morphologic patterns. Nonround/nonoval lesions were further assigned with specific morphologic patterns (Supplementary Fig. S1); c) content: solid, mixed (composite) or cystic; d) echogenicity: isohyperechoic (vs. thyroid parenchyma), mild and marked hypoechoic. The definition and schematics of the echoic content are provided in Supplementary Fig. S2; e) the presence/absence of a vascular spot and its distribution (peripheral, intranodular or both).

### Pathologic examinations

A subgroup of patients underwent cytopathology by direct smear after fine needle aspiration. Samples were stained with May-Grünwald-Giemsa and assigned to diagnostic categories according to the Bethesda system for reporting thyroid cytopathology.<sup>13</sup> A subgroup of patients underwent surgical excision of PPGs, and thus, a histopathologic examination was available. All patients underwent surgical excision in the same Institution. We carefully analyzed individual perioperative patient records to assess the matching between the US and the operative findings. We assigned the excised lesions into the following categories: a) typical (or chief cell) adenoma; b) multiglandular multiple parathyroid adenomas; c) atypical parathyroid tumor; d) parathyroid hyperplasia; and e) oncocytic adenoma (Table 1).

### Biochemical and hormone assays

Serum intact PTH was measured using a chemiluminescent immunometric assay (Centaur, Siemens, Deerfield, USA). The intra- and interassay coefficients of variation (CVs) were 2.8% and 4.6%, respectively, for 50.3 ng/L. The lower limit of detection was 4.6 ng/L.

Intranodular PTH measurement (PTHis) was measured after rinsing fine needle aspirates in 1000  $\mu$ L 0.9% NaCl aqueous solutions, as previously reported.<sup>11</sup> The specificity was set at 100% (95% CI 94.1–100.0), and the positive predictive value was set at 100%, indicating that a measurable PTHis at any level affirmed the parathyroid nature of the lesion.<sup>11</sup>

Serum calcium, phosphates and 25-hydroxy vitamin D levels were measured with routine laboratory methods. Normal ranges for serum PTH were 18.5–88.0 ng/L, calcium 2.20–2.55 mmol/L, phosphates 0.80–1.45 mmol/L, and 25-hydroxyvitamin D 30–100 ng/mL.

To establish proper correlations between the biochemical parameters and imaging findings, we carefully searched for the maximal calcium with concomitant PTH levels at the individual level in the patients' charts before any medical or nonmedical intervention (such as hyperhydration or administration of calcium sensing receptor modulators, bisphosphonates or denosumab).

### Statistical analyses

Statistical analyses and graphics were performed using the GraphPad Prism 6.01 package (GraphPad Prism, La Jolla, CA, USA). Data are expressed as individual points, as the median (interquartile range (IQR)) or mean  $\pm$  standard deviation, or as a number (percentage), as appropriate, in the text, figures and tables. Continuous variables, like tumor size and volume, were first submitted to the Anderson–Darling normality test; as they were assessed as nonnormally distributed, nonparametric tests were used to compare means between PPGs and thyroid nodules. Similarly, comparisons of maximal diameter and volume mean ranks between parathyroid adenomas and other parathyroid neoplasms subtypes were performed by Mann–Whitney tests. Comparisons between two groups were performed by Mann–Whitney tests. Comparisons of morphologic patterns, echoic content, texture content and rate and type of vascular signal between PPGs and thyroid nodules were made by means of chi-square or Fisher's tests. These tests were also employed to conduct contingency analyses with 95% confidence interval. Spearman's rank procedures were carried out to define correlations between variables. Statistical significance was set at  $p < 0.05$ .

### Role of funding source

The French Regional Health Agency (Agence Régionale de Santé Ile-de-France) CYTO-TRAIN funding source partially covered expenses for the US workstation hardware and implementations, as well as the purchase of supplies.

## Results

### Main characteristics of pathologic parathyroid glands (PPGs)

From consecutive patients undergoing neck US examination for primary and secondary/tertiary hyperparathyroidism, we validated 176 lesions from 158 patients, 66.5% of whom were women, with a median age at inclusion of 58 years (interquartile range (IQR): 43–71) (Fig. 1, Supplementary Table S1). The median maximal diameter of the parathyroid neoplasms was 12.9 mm (IQR: 8.8–16.9), and their volume was 0.34 mL (IQR: 0.14–0.88, Table 1, Table 2). In these patients, the median serum calcium concentration was 2.91 mmol/L (IQR: 2.74–3.05), and the median PTH concentration

		Reference range
<b>Etiologies (patients, n = 158)</b>		
Sporadic adenoma (unique)	111 (70.3)	
Sporadic adenoma (multiple) <sup>a</sup>	9 (5.7)	
MEN1	16 (10.1)	
MEN2	1 (0.8)	
CDC73/HRPT2	2 (1.3)	
Long-term lithium treatment	3 (1.9)	
Tertiary hyperparathyroidism (ESRD)	16 (10.1)	
<b>Biochemical parameters (patients, n = 158)</b>		
Serum calcium (mmol/L)	2.91 (2.74–3.05)	2.20–2.55
Serum albumin (g/L)	44 (41–47)	35–50
Serum phosphate (mmol/L)	0.86 (0.71–1.0)	0.80–1.45
Serum PTH (ng/L)	173 (112–296)	19–88
Serum 25-hydroxy vitamin D (ng/mL)	23 (14–31)	30–100
Serum creatinine (μmol/L)	76 (60–94)	62–110
Urinary calcium (mmol/24 h)	6.28 (4.1–9.7)	1.5–7.5
Urinary phosphates (mmol/24 h)	22.7 (14.8–32.9)	16–32
<b>Cervical location (lesions, n = 176)</b>		
Upper right (r-P4)	37 (21.0)	
Lower right (r-P3)	57 (32.4)	
Upper left (l-P4)	37 (21.0)	
Lower left (l-P3)	39 (22.2)	
Ectopic (intrathyroid)	2 (1.1)	
Ectopic (extrathyroid)	4 (2.3)	
<b>Cytopathologic examinations (lesions, n = 30)</b>		
Suggestive of PPGs	13 (43.3)	
Suggestive of thyroid neoplasms	6 (20.0)	
Undetermined nature	11 (36.7)	
<b>Histopathologic examinations (lesions, n = 128)</b>		
Parathyroid adenoma (chief cells)	88 (68.8)	
Multiglandular adenomatous disease	18 (14.1)	
Parathyroid hyperplasia	14 (10.9)	
Atypical parathyroid tumor	6 (4.7)	
Oncocytic adenoma	1 (0.8)	

Data are expressed as medians (IQ ranges) or as numbers (percentages). ESRD: end-stage renal disease. <sup>a</sup>All patients harboring multiple parathyroid lesions reported herein had no germline mutations in the *MEN1*, *RET* and *CDC73/HRPT2* genes.

**Table 1: Etiologies and main characteristics of the parathyroid lesions and laboratory data of the patients included in this study.**

was 174 ng/L (IQR: 113–288, Table 1). Most patients had sporadic tumors (single or multiple, 76.0%) (Table 1). Etiologies and other characteristics are reported in Table 1. The large majority of lesions (96.6%) were orthotopic, with six ectopic glands (2 within the thyroid gland and 4 in extrathyroidal locations, Table 1).

Histopathologic examination, available for 128 neoplasms, revealed that the majority of them were chief cell parathyroid adenomas (68.8%) (Table 1).

### Ultrasound (US) comparisons between PPG and matched thyroid nodules

From 1138 patients referred for thyroid nodules undergoing neck US examination from 2016 to 2022, we

selected 232 size/volume-matched lesions from 204 sex/age-matched patients (Table 2, Table 3, Fig. 1, Supplementary Table S1). No phosphocalcic abnormalities were found in patients carrying thyroid nodules, except vitamin D deficiency, whose prevalence was comparable to that in patients with hyperparathyroidism (Supplementary Table S1). The distribution of US characterization according to the EU-TIRADS RSS was scattered among thyroid nodules (Table 2). On cytology, most nodules were benign (44%), and 13.2% were malignant or suspicious for papillary neoplasm (Table 2). Other cytopathologic categories according to the Bethesda scoring system are provided in Table 2.

Morphologic patterns were very different between parathyroid and thyroid neoplasms. Thyroid nodules were prevalently oval or round (pooled prevalence: 84.5%), which strikingly contrasted with PPGs (44.3%,  $p < 0.0001$ , Table 3 and Fig. 2a). Specific morphologic patterns, such as flattened, reniform, triangular and dacryoid subtypes, were significantly different between parathyroid and thyroid nodules, with maximal differences for dacryoid and triangular shapes ( $p < 0.0001$  for both comparisons, Table 3 and Supplementary Fig. S1). In contrast, other minor complex morphologic shapes, such as multilobulated or spiculated edges, were not different between the two groups (Table 3 and Supplementary Fig. S1).

The echic content was also very different between parathyroid and thyroid nodules. The distribution of thyroid nodules was scattered among isoechoic, mild or marked hypoechoic and anechoic lesions (Table 3). In contrast, PPGs appeared to be more prevalently mildly (40.4%) or markedly (57.8%) hypoechoic ( $p < 0.0001$  for all comparisons, Fig. 2b). The majority of parathyroid and thyroid nodules appeared homogeneous with solid contents (63.1% vs. 56.7%, respectively,  $p = 0.22$ , Fig. 2c). Nevertheless, purely or largely cystic lesions were rarely found in PPGs (2.8%) compared to thyroid nodules (15.6%,  $p < 0.0001$ , Table 3).

We evaluated the presence and type of vascular signals in the two groups of lesions. Overall, the presence of any type of vascular signal was not different between parathyroid (69.2%) and thyroid nodules (63.5%,  $p = 0.22$ , Table 3). When analyzing the distribution of vascular signals, peripheral vascularization was not found to be more prevalent in thyroid nodules (50.7%) than in PPGs (38.5%,  $p = 0.03$ ). Intranodular vascularization, in contrast, was more frequent in PPGs (55.1%) than in thyroid nodules (30.3%,  $p < 0.0001$ , Table 3, Fig. 2d).

We analyzed the predictive values of individual or pooled US characteristics to discriminate between thyroid and parathyroid lesions (Table 4). Taken as individual parameters, nonoval shape, marked hypoechoic and intranodular vascular signals all distinguished thyroid nodules from parathyroid nodules ( $p < 0.001$  for all comparisons, Table 4). Pooled

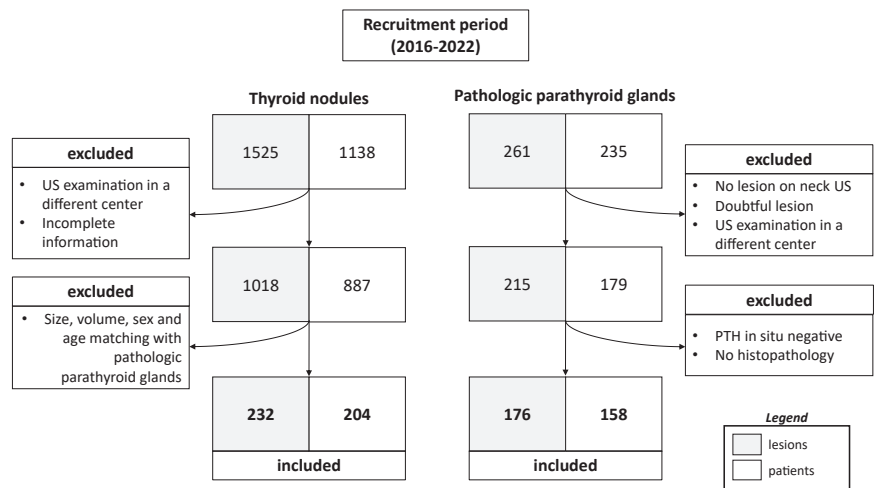


Fig. 1: Flowchart of the study population.

parameters, however, provided better odds ratios and PPVs (Table 4). The maximal OR and PPV were obtained when summing all parameters (OR 7.6; 95% CI: 3.4–17.1, PPV 93%; 95% CI: 93–98, Table 4).

PPGs were found to frequently harbor high-risk features (Fig. 2e and f). Indeed, a nonoval shape, marked hypoechoogenicity and intranodular vascular spots were all more prevalent in parathyroid than in thyroid nodules ( $p < 0.0001$  for all comparisons, Fig. 2a–f). Conversely, the homogeneous and solid contents did not differ between the two groups ( $p = 0.22$ , Fig. 2c). The presence of at least two or three high-risk features among nonoval shapes, marked hypoechoogenicity and intranodular

vascular spots were all significantly higher in parathyroid nodules than in thyroid nodules (Fig. 2e and f). Overall, high-risk scores affected 58–63% of PPGs, according to the different RSSs.

### Subgroup comparisons in patients with parathyroid tumors

Four lesions in patients carrying *CDC73/HRPT2* variants were all adenomas on histopathology. Serum calcium levels were higher in patients with parathyroid adenomas ( $3.1 \pm 0.43$  mmol/L) than in those with parathyroid hyperplasia ( $2.74 \pm 0.21$  mmol/L,  $p = 0.03$ ). Conversely, serum PTH levels were lower in patients with parathyroid adenomas ( $414 \pm 638$  ng/L) than in those with hyperplasia ( $850 \pm 747$  ng/L,  $p = 0.01$ ).

Parathyroid adenomas had larger diameters ( $16.8 \pm 9.6$  mm) and volumes ( $1.79 \pm 4.22$  mL) than multiglandular PPGs and hyperplasias ( $11.8 \pm 5.9$  mm and  $0.57 \pm 0.75$  mL,  $p = 0.013$  and  $p = 0.029$ , respectively, Fig. 3a and b). We failed to show any difference in morphological patterns between adenomas and multiglandular PPGs and hyperplasias (i.e., nonoval shape was observed in 46.4% and 55.3%, respectively), as well as in the echoic content (61.4% vs. 55.6%, respectively) or texture. In contrast, the absence of vascular spots of any type was more prevalent in hyperplastic or multiglandular adenomas (54.2%) than in adenomas (19.7%,  $p = 0.0032$ , Fig. 3c). In addition, intranodular vascular signals were more prevalent in adenomas (68.4%) than in hyperplasias or multiglandular adenomas (33.0%,  $p = 0.0037$ , Fig. 3c). Atypical parathyroid tumors were larger than chief cell adenomas (maximal diameter  $39.1 \pm 9.2$ ,  $p < 0.0001$ , Fig. 3d).

Maximal parathyroid tumor diameter and volumes did not differ between patients with and without type-1 multiple endocrine neoplasia. Lesions from patients harboring mutations in the *CDC73/HRPT2* gene

Sex, F (%)	132 (64.7)
Age at inclusion (yrs)	60 (47–68)
Serum TSH (mIU/L)	1.43 (1.09–1.86)
Serum calcium (mmol/L)	2.34 (2.28–2.44)
<b>EU-TIRADS score</b>	<b>n = 232</b>
2	50 (21.5)
3	81 (34.9)
4	53 (22.8)
5	48 (20.7)
<b>Bethesda cytopathology scoring system</b>	<b>n = 68</b>
I	9 (13.2)
II	30 (44.1)
III	7 (10.3)
IV	13 (19.1)
V	5 (7.3)
VI	4 (5.9)

Data are expressed as medians (IQ ranges) or as numbers (percentage). For more detail about EU-TIRADS RSSs, please see Russ G et al.<sup>13</sup>

**Table 2: Main demographic, biological, US characteristics and cytopathology of patients with thyroid nodules included in this study.**

	Pathologic parathyroid glands n = 176	Thyroid nodules n = 232	p
Maximal diameter, mm	12.9 (8.8–16.9)	13.0 (9.9–17.0)	NS
Volume, mL	0.34 (0.14–0.88)	0.47 (0.23–1.07)	NS
Morphology <sup>a</sup>	(n = 167)	(n = 232)	
Round	5 (3.0)	45 (19.4)	<0.0001
Oval	69 (41.3)	151 (65.1)	<0.0001
Kidney-shaped	13 (7.8)	5 (2.2)	0.0124
Dacryoid (eye-shaped)	14 (8.4)	1 (0.4)	<0.0001
Flat	21 (12.6)	8 (3.4)	0.0007
Triangular	26 (15.6)	6 (2.6)	<0.0001
Other morphological patterns (various) <sup>a</sup>	19 (11.4)	16 (6.9)	NS
Echogenicity <sup>b</sup>	(n = 166)	(n = 232)	
Anechoic (pure cyst)	0 (0.0)	36 (15.5)	<0.0001
Isoechoic/hyperechoic (vs. thyroid)	3 (1.8)	89 (38.4)	<0.0001
Mild hypoechoic	67 (40.4)	47 (20.3)	<0.0001
Marked hypoechoic	96 (57.8)	60 (25.9)	<0.0001
Texture	(n = 176)	(n = 231)	
Homogeneous (solid)	111 (63.1)	131 (56.7)	NS
Heterogeneous	60 (34.1)	64 (27.7)	NS
Largely cystic	5 (2.8)	36 (15.6)	<0.0001
Vascular spot	(n = 156)	(n = 211)	
Yes (any type)	108 (69.2)	134 (63.5)	NS
Peripheral <sup>c</sup>	60 (38.5)	107 (50.7)	0.03
Intranodular <sup>c</sup>	86 (55.1)	64 (30.3)	<0.0001

Data are expressed as medians (IQR) or as numbers (percentages). NS: nonsignificant. <sup>a</sup>For more detail concerning morphologic characteristics and definitions, please see [Supplementary Fig. S1](#). <sup>b</sup>Further details on the definition of echogenic patterns are reported in [Supplementary Fig. S2](#). <sup>c</sup>Includes peripheral (or intranodular) plus mixed (peripheral + intranodular).

**Table 3: Comparison of the ultrasound characteristics between parathyroid and thyroid lesions.**

tended to be larger than sporadic lesions (n = 4, 25.3 ± 12.9 mm vs. 14.5 ± 9.0 mm, p = 0.053).

No differences in size, volume or US characteristics were found according to the location (upper or lower glands, or orthotopic vs. ectopic).

### Bioradiological correlations

Correlation analyses between calcium or PTH levels and the size and volume of PPGs were conducted only in patients with primary hyperparathyroidism harboring single lesions. Thus, we excluded patients with multiple adenomas, those with a predisposing germline genetic disease and those with end-stage kidney failure from this analysis. Serum calcium concentrations were correlated with the maximal diameter lesion (r = 0.58, p < 0.0001, [Fig. 4a](#)) and with the calculated parathyroid volumes (r = 0.59, p < 0.0001, [Fig. 4b](#)). Serum PTH levels were also correlated with maximal PPG diameter (r = 0.58, p < 0.0001, [Fig. 4c](#)) and with parathyroid volume (r = 0.66, p < 0.0001, [Fig. 4d](#)). No correlation was found between lesion diameters or volumes and serum phosphate, daily urinary calcium and phosphates (data not shown). We compared bioradiologic correlations with those previously reported ([Table 5](#)). The majority of studies revealed a significant correlation between tumor sizes and circulating calcium or PTH levels. However,

when comparing previous reports, we found the highest coefficient correlations concerning the relationship between serum calcium and tumor size and volume and between serum PTH and tumor diameter ([Table 5](#)).

### Discussion

Primary hyperparathyroidism and thyroid nodules are two highly prevalent disorders in the general population. Ultrasound-based imaging represents the first-line technique to characterize cervical masses. High-performing devices have been developed with high spatial resolution and advanced tools to accurately define the nodular size, shape, structural content and vascular status. Beyond radiological settings, US devices have been successfully used in different medical settings, such as in emergency departments and in various medical specialties, including primary care.<sup>9</sup>

When evaluating thyroid nodules, various US-based RSSs have been developed to stratify the risk of malignancy and to establish the requirement and appropriateness of conducting fine needle aspiration or core needle biopsy for cytopathological studies.<sup>7,8,14,22</sup> Although RSSs are primarily focused on predicting papillary neoplasms, variable performances are available for other cervical lesions and thyroid malignancies.<sup>23</sup>

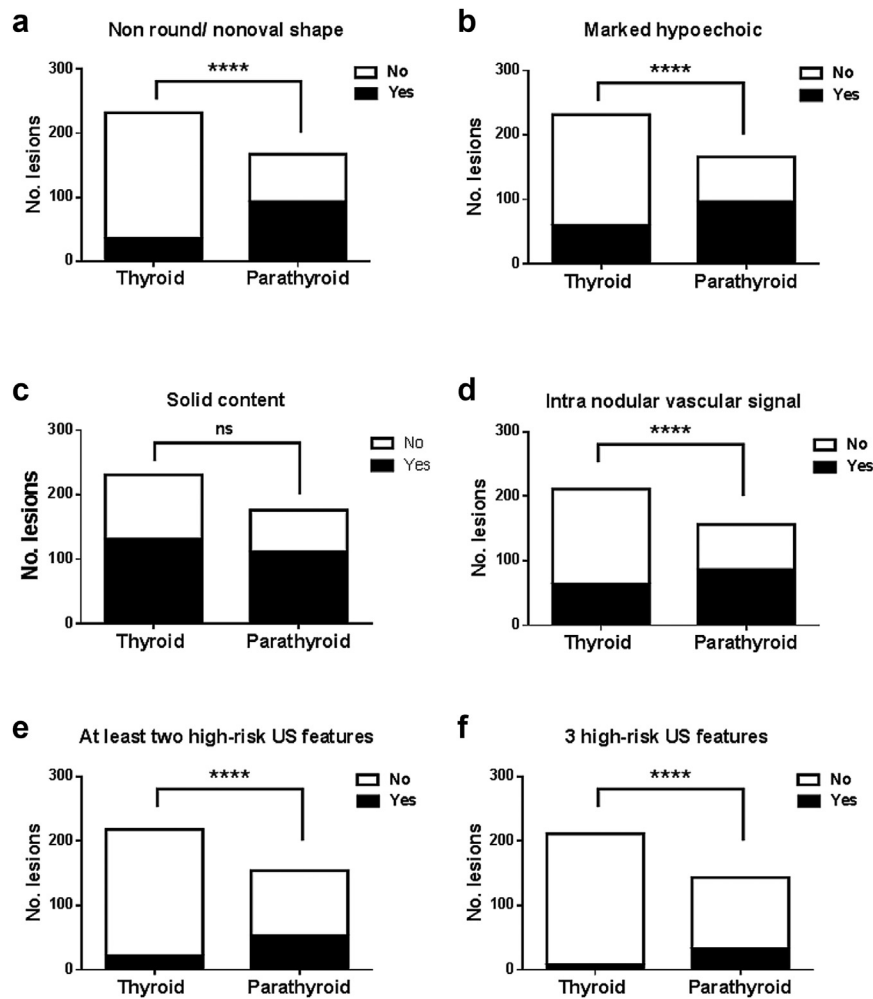


**Fig. 2: US characteristics in thyroid vs. parathyroid lesions.** a) Number of lesions with or without a round/oval shape; b) Number of lesions with or without marked hypoechoic content; c) Number of lesions with or without solid content; d) Number of lesions with or without an intranodular vascular signal; e) Number of lesions with or without the association of two or more high-risk US features according to the EU-TIRADS risk stratification system<sup>14</sup>; f) Number of lesions with or without the association of three high-risk US features according to the EU-TIRADS risk stratification system.<sup>14</sup> \*\*\*\*p < 0.0001.

	p	OR (CI 95%)	Sensitivity (CI 95%)	Specificity (CI 95%)	PPV (CI 95%)	NPV (CI 95%)
<b>1 parameter</b>						
Nonround/non oval shape (A)	<0.0001	6.8 (4.3-10.9)	72.6 (67-78)	72.1 (64-80)	84 (79-89)	56 (48-63)
Markedly hypoechoic (B)	<0.0001	3.9 (2.6-6.0)	71.1 (65-77)	61.5 (53-69)	74 (68-80)	58 (50-65)
Intranodular vascular signal (C)	<0.0001	3.1 (2.0-4.8)	69.7 (63-76)	57.3 (49-65)	70 (63-76)	57 (49-65)
<b>2 parameters</b>						
A + B	<0.0001	6.4 (3.5-11.5)	66 (61-71)	76 (65-86)	93 (88-96)	34 (26-41)
A + C	<0.0001	3.9 (2.3-6.7)	66 (60-72)	67 (55-77)	88 (82-92)	35 (28-44)
B + C	<0.0001	4.1 (2.4-7.1)	65 (59-71)	69 (57-79)	89 (84-93)	35 (27-43)
<b>3 parameters</b>						
A + B + C	<0.0001	7.6 (3.4-17.1)	65 (59-70)	80 (65-91)	96 (93-98)	23 (16-31)

OR: odds ratio (parathyroid vs. thyroid); PPV: positive predictive value; NPV: negative predictive value.

**Table 4: Performance of parameter combinations to discriminate parathyroid from size- and volume-matched thyroid lesions.**

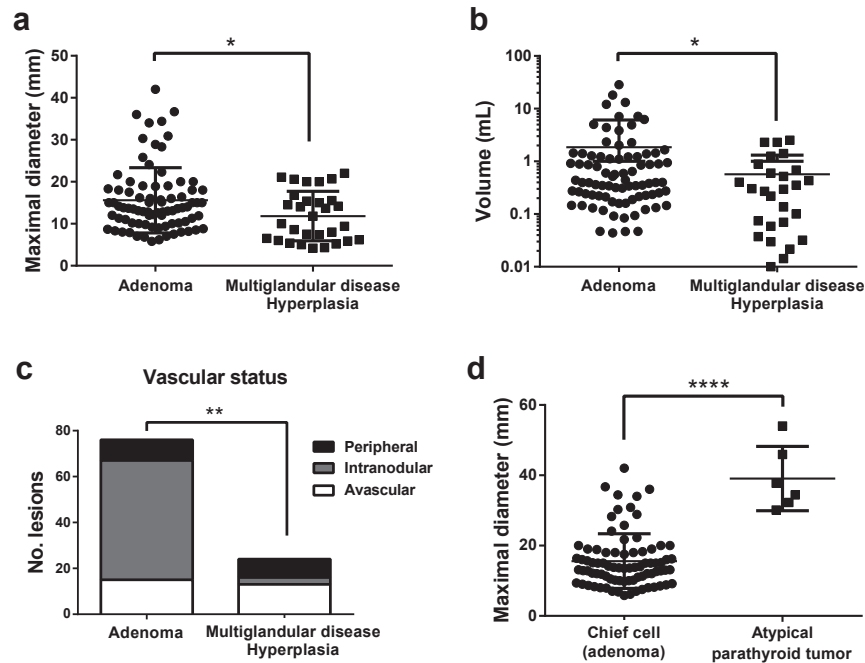


**Fig. 3:** US characteristics in different subgroups of abnormal parathyroid glands. a) Mean maximal tumor diameter compared between parathyroid adenomas and hyperplasia; b) Mean tumor volume compared between parathyroid adenomas and hyperplasia; c) Number of lesions with or without an overall and specific (intranodular or peripheral) vascular signal; d) Mean maximal tumor diameter compared between typical (chief cell) and atypical parathyroid adenoma. \* $p < 0.05$ ; \*\* $p < 0.01$ ; \*\*\*\* $p < 0.0001$ .

Parathyroid imaging is required to refine the clinical work-up in patients with hyperparathyroidism and thereby assist surgeons in preoperatively locating PPGs. Among various imaging techniques, neck US is used with variable performance to identify abnormal parathyroid glands.<sup>20,24,25</sup> Indeed, cervical US is an easily available, noninvasive, nonirradiating and cost-effective procedure, allowing the detection of PPG in addition to coexisting thyroid nodules, which may be managed concurrently.<sup>2</sup> Neck US has even been proposed as the primary imaging technique in a stepwise approach in localizing abnormal parathyroid glands.<sup>26</sup> PPGs on US are usually described as small, hypoechoic or hyperechoic oblong lesions posterior to the thyroid gland.<sup>27</sup> The diagnostic yield improves if they are located outside the thyroid capsule. In several instances, however, PPGs may be confused with thyroid nodules, especially in cases of posterior thyroid nodules, or if the procedure is performed by inexperienced or hurried operators.<sup>28–30</sup> Moreover, parathyroid glands may, albeit rarely, be found within the thyroid parenchyma.<sup>31</sup> In addition, histologically proven parathyroid adenomas have also rarely been described in the absence of any calcium-phosphate abnormalities, in the setting of incidentalomas, or as occult parathyroid adenomas.<sup>32</sup> For instance, in our cohort, up to 8% of patients with parathyroid lesions were initially referred for a cervical nodule and not for abnormalities in

calcium-phosphate homeostasis. Beyond the radiological setting, cytopathologists have also failed to discriminate parathyroid from thyroid lesions, as in one report, 24% of 143 thyroid nodule specimens with indeterminate cytology were confirmed to be parathyroid nodules on histology.<sup>5</sup> Distinguishing thyroid nodules from PPGs therefore represents an important issue for radiologists and for a wide community of point-of-care US operators.<sup>33,34</sup>

Our exploratory findings reveal the presence of distinct morphological characteristics of PPGs. Contrary to thyroid nodules, in more than half of cases they appear nonround and nonoval, harboring various morphologic patterns, such as being kidney- or eye-shaped (Supplementary Fig. S1). Although we do not know the mechanisms leading to the acquisition of these morphological aspects, we speculate that enlarged parathyroid glands must adapt to the cervical loge and occupy the available space surrounding the thick thyroid capsule.<sup>28</sup> PPGs are markedly hypoechoic (i.e., grayscale lower than that of the strap muscles). Some authors suggest that the hypoechoic signal on US is the result of marked, compact cellularity.<sup>4</sup> The intranodular vascular signal is more frequent in abnormal parathyroid glands than in size-matched thyroid nodules. We selected size- and volume-matched thyroid nodules because it is known that the shape, content and vascular status significantly depend on the nodular size.<sup>35,36</sup>



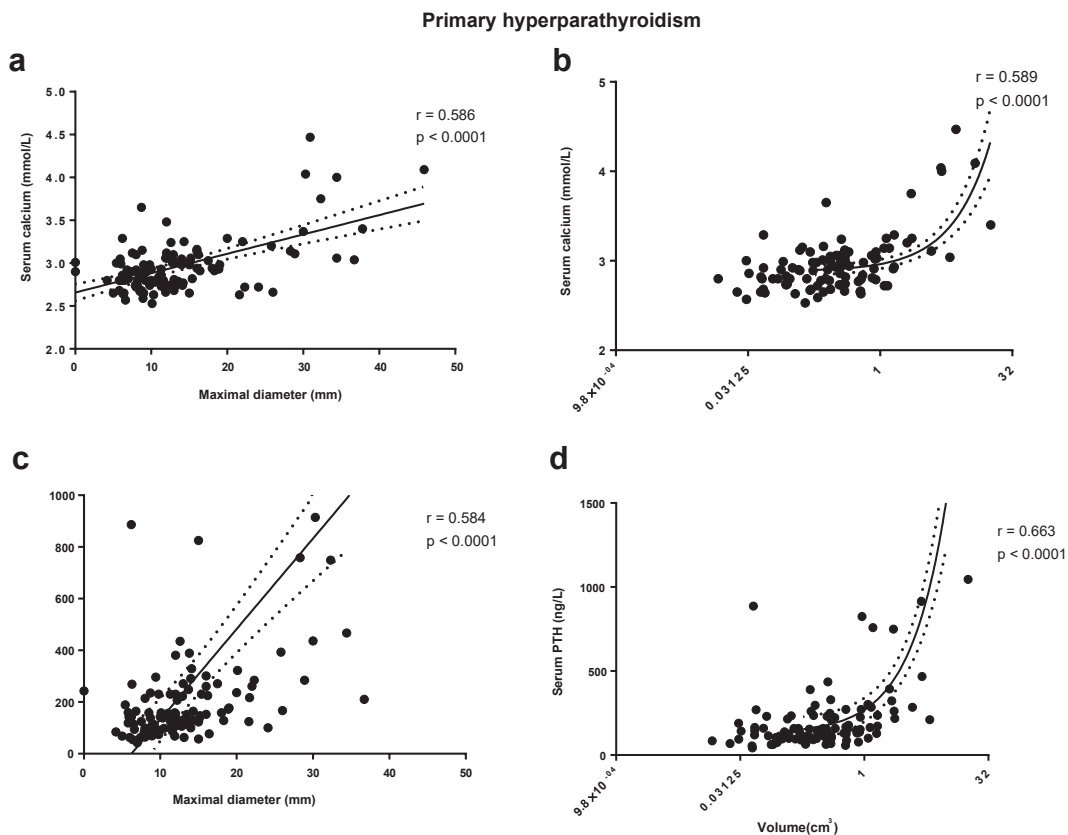


**Fig. 4: Correlation between US findings and biochemical parameters.** a) Correlation between the maximal diameter of abnormal parathyroid lesions and circulating calcium levels. b) Correlation between the tumor volume of abnormal parathyroid lesions and circulating calcium levels. Please note the log<sub>2</sub> logarithmic scale on the x-axis. c) Correlation between the maximal diameter of abnormal parathyroid lesions and circulating PTH levels. d) Correlation between the tumor volume of abnormal parathyroid lesions and circulating PTH levels. Please note the log<sub>2</sub> logarithmic scale on the x-axis. Data are represented as linear regressions with 95% confidence intervals.

In a further step, we tested the performances of US parameters, alone or in combination. The combination of nonoval shape, marked hypoechoic content and intranodular vascular spot improved the OR and the positive predictive value of dealing with PPG.

PPGs carry a significant risk of being misclassified as high-risk nodules when adopting a thyroid-based RSS.<sup>37,38</sup> Indeed, beyond microcalcifications and irregular borders, which were not observed in parathyroid nodules, approximately 60% of parathyroid lesions bear at least one or more high-risk US characteristics based on common RSSs.<sup>14,22</sup>

Another aim of the PARATH-US study was to perform bioradiologic correlations. We found a positive relationship between parathyroid size and either calcium or PTH levels. These findings suggest that the more severe the phosphocalcic abnormality, the larger the pathologic lesion is likely to be. Although our study was not specifically designed to test the diagnostic accuracy of US to locate PPG, it seems pertinent to speculate that the likelihood of finding PPGs on US may

increase in patients with high calcium or PTH levels. Previous studies have reported correlations between parathyroid size or weight and peripheral calcium or PTH levels.<sup>17,21,39</sup> However, compared with previous reports, we found the highest correlation coefficients. We collected calcium and PTH levels before any medical or nonmedical (i.e., hyperhydration) intervention. Furthermore, we excluded patients with multiple adenomas (each of which may differently contribute to the systemic PTH and calcium pool), as well as those with genetic diseases predisposing to the occurrence of multiple parathyroid lesions (germ line mutations in *MEN1*, *RET* and *CDC73/HRPT2* genes). Last, we excluded patients with kidney failure, in whom renal hydroxylation to activated 1,25 dihydroxy (1,25-OH) vitamin D is impaired, and in whom calcium and PTH levels would have been under- and overestimated, respectively.<sup>40</sup> Indeed, serum calcium levels were lower and PTH levels were higher in patients with tertiary hyperparathyroidism than in those with primary hyperparathyroidism.

Serum PTH vs. maximal diameter	N	r	p
Wang et al. 1995 <sup>15</sup>	68	0.334	0.002
Al Faifi et al. 2018 <sup>16</sup>	35	0.29	0.095
Current study	111	0.584	<0.001
Serum PTH vs. tumor volume	N	r	p
Wang et al. 1995 <sup>15</sup>	–	0.334	0.002
Bindlish et al. 2002 <sup>17</sup>	63	0.462	0.001
Hwang-Bo et al. 2011 <sup>18</sup>	68	0.155	0.208
Kamani et al. 2012 <sup>19</sup>	69	0.327	0.006
Filser et al. 2021 <sup>20</sup>	138	0.342	<0.001
Rezkallah et al. 2023 <sup>21</sup>	99	0.708	<0.01
Current study	111	0.663	<0.001
Serum calcium vs. maximal diameter	N	r	p
Al Faifi et al. 2018 <sup>16</sup>	35	–0.033	0.85
Current study	111	0.586	<0.001
Serum calcium vs. tumor volume	N	r	p
Bindlish et al. 2002 <sup>17</sup>	63	0.542	0.004
Hwang-Bo et al. 2011 <sup>18</sup>	68	–0.037	0.765
Kamani et al. 2012 <sup>19</sup>	69	0.333	0.005
Filser et al. 2021 <sup>20</sup>	138	0.295	<0.001
Rezkallah et al. 2023 <sup>21</sup>	99	0.329	<0.01
Current study	111	0.589	<0.001

N: number of subjects; r: correlation coefficients of linear regressions.

**Table 5: Correlation analyses of biochemical parameters vs. tumor size compared with previous reports.**

We also provide the first description of US characteristics across different subgroups of patients with hyperparathyroidism. The tumor sizes and volumes were higher in patients with chief cell adenomas than in those with multiglandular disease and parathyroid hyperplasia. Atypical parathyroid tumors were larger than chief cell adenomas.

The main strength of the PARATH-US study lies in methodology. We compared well-characterized and genotyped PPG to size- and volume-matched thyroid nodules in an attempt to attenuate any bias resulting from nodular size.<sup>41</sup>

Some limitations, however, deserve to be mentioned. Comparative analyses in patient subgroups, particularly in those harboring genetic mutations, may have failed because of the small sample size. We did not provide elastometric measures, as these procedures were not conducted on a systematic basis in our cohort. Importantly, we did not perform contrast-enhanced US, a technique that has proven highly useful to diagnose and locate PPGs, especially to explore the vascular architecture.<sup>42,43</sup> Furthermore, given the nature of our samples, we were not able to perform specific PTH or GATA-3 staining or PTH mRNA quantification on cytopathology, which are useful complementary techniques to help distinguishing thyroid from parathyroid tissues.<sup>44</sup>

In conclusion, we demonstrate that parathyroid lesions have specific US characteristics. This study may

help radiologists and clinicians find clues to discriminate parathyroid lesions from thyroid nodules. PPGs, if confused with thyroid nodules, are enriched with suspicious US features according to the commonly adopted RSSs. In the presence of elongated lesions with marked hypoechoic content and intranodular vascular spots, PPGs should be suspected, and the assessment of serum calcium and PTH levels should be recommended to rule out hyperparathyroidism and to avoid unnecessary invasive diagnostic and therapeutic procedures.

**Contributors**

Study conceptualization (DY, LM); study management and administration (DY, PK, JY); design of methodology (DY, CR, JY, PC, LM); enrolment of patients (SS, PK, AB, LC, JFP, JY, PC, LM); neck US examinations (CR, LM); neck US fine-needle aspirations (CR, LM); data collection and cleaning (DY, CR, MD, LM); data analyses (DY, SS, LC, AB, PC, LM); study drafting (DY, MD, PC); final revisions (PC, LM). All authors were not precluded from having full access to all the data collected in the PARATH-US study and accepted responsibility to the current submission.

**Data sharing statement**

Data generated or analyzed during the study are available from the corresponding author by request.

**Declaration of interests**

None declared.

**Acknowledgements**

We greatly thank Mr Tristan Verdelet for his assistance in the study and academic management for the PARATH-US study.

Funding information: PARATH-US study has been funded in part by the Interventional Regional Fund (FIR) “CYTO-TRAIN”, reference number C2022DOSRH053, funded by the French Regional Health Agency (Agence Régionale de Santé Ile-de-France).

**Appendix A. Supplementary data**

Supplementary data related to this article can be found at <https://doi.org/10.1016/j.lanepc.2023.100751>.

**References**

- Walker MD, Silverberg SJ. Primary hyperparathyroidism. *Nat Rev Endocrinol.* 2018;14(2):115–125.
- Hindie E, Schwartz P, Avram AM, Imperiale A, Sebag F, Taieb D. Primary hyperparathyroidism: defining the appropriate preoperative imaging algorithm. *J Nucl Med.* 2021;62(Suppl 2):3S–12S.
- Cakir B, Cuhaci Seyrek FN, Topaloglu O, et al. Ultrasound elastography score and strain index in different parathyroid lesions. *Endocr Connect.* 2019;8(12):1579–1590.
- Johnson NA, Tublin ME, Ogilvie JB. Parathyroid imaging: technique and role in the preoperative evaluation of primary hyperparathyroidism. *AJR Am J Roentgenol.* 2007;188(6):1706–1715.
- Cho M, Oweity T, Brandler TC, Fried K, Levine P. Distinguishing parathyroid and thyroid lesions on ultrasound-guided fine-needle aspiration: a correlation of clinical data, ancillary studies, and molecular analysis. *Cancer Cytopathol.* 2017;125(9):674–682.
- Dean DS, Gharib H. Epidemiology of thyroid nodules. *Best Pract Res Clin Endocrinol Metab.* 2008;22(6):901–911.
- Borson-Chazot F, Buffet C, Decaussin-Petrucci M, et al. SFE-AFCE-SFMN 2022 consensus on the management of thyroid nodules: synthesis and algorithms. *Ann Endocrinol (Paris).* 2022;83(6):440–453.
- Haugen BR, Alexander EK, Bible KC, et al. 2015 American thyroid association management guidelines for adult patients with thyroid nodules and differentiated thyroid cancer: the American thyroid association guidelines task force on thyroid nodules and differentiated thyroid cancer. *Thyroid.* 2016;26(1):1–133.
- Andersen CA, Holden S, Vela J, Rathleff MS, Jensen MB. Point-of-Care ultrasound in general practice: a systematic review. *Ann Fam Med.* 2019;17(1):61–69.

- 10 Brandenstein M, Wiesinger I, Kunzel J, Hornung M, Stroszczynski C, Jung EM. Multiparametric sonographic imaging of thyroid lesions: chances of B-mode, elastography and CEUS in relation to preoperative histopathology. *Cancers (Basel)*. 2022;14(19):4745.
- 11 Richa C, Haidar H, Dupeux M, et al. Parathyroid hormone in situ measurement in patients with hyperparathyroidism: single-centre experience of 179 patients. *Eur J Endocrinol*. 2022;186(4):489–501.
- 12 Yamashita Y, Yoshikawa T, Kawaji Y, et al. Novel endoscopic ultrasonography imaging technique for visualizing microcirculation without contrast enhancement in subepithelial lesions: prospective study. *Dig Endosc*. 2021;33(6):955–961.
- 13 Cibas ES, Ali SZ. The 2017 Bethesda system for reporting thyroid cytopathology. *Thyroid*. 2017;27(11):1341–1346.
- 14 Russ G, Bonnema SJ, Erdogan MF, Durante C, Ngu R, Leenhardt L. European thyroid association guidelines for ultrasound malignancy risk stratification of thyroid nodules in adults: the EU-TIRADS. *Eur Thyroid J*. 2017;6(5):225–237.
- 15 Wang M, Hercz G, Sherrard DJ, Maloney NA, Segre GV, Pei Y. Relationship between intact 1-84 parathyroid hormone and bone histomorphometric parameters in dialysis patients without aluminum toxicity. *Am J Kidney Dis*. 1995;26(5):836–844.
- 16 Al Faiji J. Correlations between parathyroid hormone level, adenoma size, and serum calcium level in patients with primary hyperparathyroidism. *Saudi Surg J*. 2018;6(4):122–125.
- 17 Bindlish V, Freeman JL, Witterick IJ, Asa SL. Correlation of biochemical parameters with single parathyroid adenoma weight and volume. *Head Neck*. 2002;24(11):1000–1003.
- 18 Hwang-Bo Y, Kim JH, An JH, et al. Association of the parathyroid adenoma volume and the biochemical parameters in primary hyperparathyroidism. *Endocrinol Metab*. 2011;26(1):62–66.
- 19 Kamani F, Najafi A, Mohammadi SS, Tavassoli S, Shojaei SP. Correlation of biochemical markers of primary hyperparathyroidism with single adenoma weight and volume. *Indian J Surg*. 2013;75(2):102–105.
- 20 Filser B, Usler V, Weyhe D, Tabriz N. Predictors of adenoma size and location in primary hyperparathyroidism. *Langenbecks Arch Surg*. 2021;406(5):1607–1614.
- 21 Rezkallah E, Elsaify A, Hanna R, Elsaify W. Correlation between preoperative calcium and parathormone levels with parathyroid gland volume. *Endocr Regul*. 2023;57(1):12–17.
- 22 Shin JH, Baek JH, Chung J, et al. Ultrasonography diagnosis and imaging-based management of thyroid nodules: revised Korean society of thyroid radiology consensus statement and recommendations. *Korean J Radiol*. 2016;17(3):370–395.
- 23 Matrone A, Gambale C, Biagini M, Prete A, Vitti P, Elisei R. Ultrasound features and risk stratification systems to identify medullary thyroid carcinoma. *Eur J Endocrinol*. 2021;185(2):193–200.
- 24 Gurney TA, Orloff LA. Otolaryngologist-head and neck surgeon-performed ultrasonography for parathyroid adenoma localization. *Laryngoscope*. 2008;118(2):243–246.
- 25 Steward DL, Danielson GP, Afman CE, Welge JA. Parathyroid adenoma localization: surgeon-performed ultrasound versus sestamibi. *Laryngoscope*. 2006;116(8):1380–1384.
- 26 Korwar V, Yuen Chang F, Teasdale E, Suchett-Kaye I, Edwards A, Morgan J. Stepwise approach for parathyroid localisation in primary hyperparathyroidism. *World J Surg*. 2020;44(3):803–809.
- 27 Itani M, Middleton WD. Parathyroid imaging. *Radiol Clin North Am*. 2020;58(6):1071–1083.
- 28 Moccia MC, Miller EE, Vaz CL. Occult primary hyperparathyroidism: a case report and review of parathyroid ultrasonography. *AACE Clin Case Rep*. 2020;6(3):e127–e131.
- 29 Morris MA, Saboury B, Ahlman M, et al. Parathyroid imaging: past, present, and future. *Front Endocrinol (Lausanne)*. 2021;12:760419.
- 30 Barbaros U, Erbil Y, Salmashoglu A, et al. The characteristics of concomitant thyroid nodules cause false-positive ultrasonography results in primary hyperparathyroidism. *Am J Otolaryngol*. 2009;30(4):239–243.
- 31 Hacıyanlı SG, Karaisli S, Erdogan N, Turgut B, Gur EO, Hacıyanlı M. Intrathyroidal parathyroid adenomas in primary hyperparathyroidism: clinical and imaging findings. *Sisli Etfal Hastan Tip Bul*. 2022;56(2):256–261.
- 32 Poppe K, Pipeleers-Marichal M, Flamen P, et al. Non-secreting atypical parathyroid adenoma. *J Endocrinol Invest*. 2001;24(2):107–110.
- 33 Russell MD, Orloff LA. Ultrasonography of the thyroid, parathyroids, and beyond. *HNO*. 2022;70(5):333–344.
- 34 Hashim A, Tahir MJ, Ullah I, Asghar MS, Siddiqi H, Yousaf Z. The utility of point of care ultrasonography (POCUS). *Ann Med Surg (Lond)*. 2021;71:102982.
- 35 Xie C, Cox P, Taylor N, LaPorte S. Ultrasonography of thyroid nodules: a pictorial review. *Insights Imaging*. 2016;7(1):77–86.
- 36 Ren J, Liu B, Zhang LL, et al. A taller-than-wide shape is a good predictor of papillary thyroid carcinoma in small solid nodules. *J Ultrasound Med*. 2015;34(1):19–26.
- 37 Campanella P, Ianni F, Rota CA, Corsello SM, Pontecorvi A. Quantification of cancer risk of each clinical and ultrasonographic suspicious feature of thyroid nodules: a systematic review and meta-analysis. *Eur J Endocrinol*. 2014;170(5):R203–R211.
- 38 Remonti LR, Kramer CK, Leitao CB, Pinto LC, Gross JL. Thyroid ultrasound features and risk of carcinoma: a systematic review and meta-analysis of observational studies. *Thyroid*. 2015;25(5):538–550.
- 39 Stern S, Mizrahi A, Strenov Y, et al. Parathyroid adenoma: a comprehensive biochemical and histological correlative study. *Clin Otolaryngol*. 2017;42(2):381–386.
- 40 Yuen NK, Ananthakrishnan S, Campbell MJ. Hyperparathyroidism of renal disease. *Perm J*. 2016;20(3):15–127.
- 41 Meng C, Wang W, Zhang Y, Li X. The influence of nodule size on the aggressiveness of thyroid carcinoma varies with patient's age. *Gland Surg*. 2021;10(3):961–972.
- 42 Agha A, Hornung M, Stroszczynski C, Schlitt HJ, Jung EM. Highly efficient localization of pathological glands in primary hyperparathyroidism using contrast-enhanced ultrasonography (CEUS) in comparison with conventional ultrasonography. *J Clin Endocrinol Metab*. 2013;98(5):2019–2025.
- 43 Centello R, Sesti F, Feola T, et al. The dark side of ultrasound imaging in parathyroid disease. *J Clin Med*. 2023;12(7):2487.
- 44 Erdogan-Durmus S, Ramazanoglu SR, Barut HY. Diagnostic significance of GATA 3, TTF-1, PTH, chromogranin expressions in parathyroid fine needle aspirations via immunocytochemical method. *Diagn Cytopathol*. 2023;51(7):449–454.